Vol. 13, No. 3 (2024): 637 - 649 http://dx.doi.org/10.23960/jtep-l.v13i3.637-649

JURNAL TEKNIK PERTANIAN LAMPUNG

ISSN 2302-559X (print) / 2549-0818 (online)
Journal homepage : https://jurnal.fp.unila.ac.id/index.php/JTP

Response Surface Methodology (RSM) for Optimization Carbonization Parameters of Exhausted Coffee Husk for Iron Removal from Aqueous Solution

Aninda T. Puari [1], Nika R. Yanti [1], Nurmala Sari [1], Rusnam [1,✉]

[1] Department of Agricultural and Biosystem Engineering, Faculty of Agricultural Technology, Andalas University, West Sumatera, INDONESIA.

Article History:

Received : 03 December 2023
Revised : 27 March 2024
Accepted : 17 April 2024

Keywords:

Biochar,
Biosorption capacity,
Box-Behnken design,
Temperature,
Time.

Corresponding Author:
✉ rusnam@ae.unand.ac.id

ABSTRACT

In this study, biochar derived from exhausted coffee husk (ECH) was used as biosorbent for removing Iron (II) from aqueous solution. The aim of this study was to improve the biosorption capacity of the biosorbent from agricultural solid waste and its usability for Fe^{2+} removal. The biosorption performance of ECH biochar was optimized through carbonization parameters: temperature, time, and temperature gradient. Response Surface Methodology (RSM) based on multivariate analysis was employed to evaluate the biosorption performance of ECH biochar for Fe^{2+} biosorption. The optimum performance predicted through Box-Behnken design experiment. The optimal combination of the three parameters was 549.37°C, 1.98 h and 21.98°C/min. At the optimal condition the removal efficiency (RE) was predicted to be 107.01% and biosorption capacity (qt) was 5.11 mg/g. SEM-EDX, FT-IR and XRD analysis were conducted in this study to evaluate the biosorption mechanism of ECH biochar on the iron ion. The results showed that ion exchange existed on the surface of the ECH biochar during the biosorption. Additionally, the presence of functional groups on the ECH biochar surface responsible for Fe(II) binding. Overall, the findings of this study suggested an eco-friendly strategy for optimizing the removal of Iron (II) from polluted water by the biosorption onto ECH biochar.

1. INTRODUCTION

Iron (Fe) is the most prevalent heavy metal on Earth, serving as an essential nutrient for enzymes and proteins in humans, plants, and algae (Ngah *et al*., 2005). However, its excessive presence can become toxic (Jaishankar *et al*., 2014). Elevated levels of iron in the topsoil significantly influence the behavior of phosphorus in the soil, rendering it less available to plants and soil microorganisms. This phenomenon leads to the degradation of arable land and substantial economic losses (Corral-Bobadilla *et al*., 2021; MarouŠek, 2013).

Various techniques are available for water treatment, encompassing ion exchange, reverse osmosis, adsorption, flocculation, chemical precipitation, and flotation (Fu & Wang, 2011; Mallesh, 2018; Qasem *et al*., 2021). Nevertheless, these methods can become financially burdensome due to the perpetual nature of the materials involved and the associated high operational and material costs. Notably, affordability and operational simplicity play pivotal roles when selecting an appropriate treatment method (Puari *et al*., 2022; Rusnam *et al*., 2022; Zhou *et al*., 2019). Adsorption emerges as a preferred choice due to its straightforward operation, remarkable contaminant removal efficiency, facile material recovery, renewability (in cases involving adsorbents like activated carbon), and cost-effectiveness (Gadd, 2008; Huang *et al*., 2018).

A recent study has unveiled the potential of using biochar (BC) derived from exhausted coffee husks (ECH) for the removal of Fe (II) from aqueous solutions. One of the process used for producing biochar form ECH is carbonization. The carbonization process assumes a pivotal role in fostering the creation of porous structures and active sites capable of entrapping waterborne pollutants (Prasannamedha *et al*., 2021). Notably, the carbonization process's temperature, duration, and temperature gradient significantly affect the performance of ECH-biochar concerning Fe (II) removal from water (Rusnam *et al*., 2024). However, the intricate interplay of these multiple variables has yet to be comprehensively explored. This knowledge gap results in an expensive and inefficient approach. Leveraging multivariate statistical techniques can substantially reduce the number of requisite experiments and the influence of independent variables, thereby fostering advancements in the operational framework. Moreover, optimization efforts lead to a noteworthy reduction in experimental costs (Kaçakgil & Çetintaş, 2021; Zhou *et al*., 2019). The Response Surface Methodology (RSM), a mathematical statistical approach for constructing regression models, has gained widespread adoption for identifying the optimal combination of parameters to enhance heavy metal absorption efficiency and that of its biosorbent (Bezerra *et al*., 2008; Korondi *et al*., 2021).

Regrettably, existing literatures lacks references to the application of RSM for determining the optimal combination of parameters (specifically temperature, duration, and temperature gradient) in the carbonization process, particularly concerning ECH-biochar as a biosorbent for Fe ions. The principal objective of the present study was to comprehensively optimize the carbonization process using RSM, employing biochar derived from exhausted coffee husks (ECH), to efficiently eliminate Fe ions from aqueous solutions. A Box-Behnken Design was employed in the optimization scenario, aiming to maximize biosorption capacity (*qt*) and removal efficiency (*RE*).

2. MATERIALS AND METHODS

2.1. Preparation Procedure for ECH Biochar and Standard Solutions

The exhausted coffee husks (ECH) were collected from KUPS Agroforestri Kopi Data, Agam Regency, West Sumatera. The ECH were cleaned with tap water twice prior to washing with distilled water once and dried at 105ºC for 24 hours with electric oven (MEMMERT UN 55). After the drying process, the dried ECH underwent the carbonization process in muffle furnace (Nabertherm B180). The carbonization parameters, namely temperature, time and gradient, were varied according to the Box-Behnken matrix (Table 2). The yield (*Y*) of each carbonization process with different matrix were evaluated using Equation (1):

$$Y\,(\%) = (W/W_o) \times 100\% \quad (1)$$

with W is the final weight after carbonization and W_o is the weight before carbonization.

Meanwhile, the determination of ash content (*Ash*) of the biochar(s) followed the procedure by Aller *et al*. (2017) and calculated using Equation (2) as follows:

$$Ash\,(\%) = (M_{ash}/M_{bc}) \text{ x } 100\% \quad (2)$$

where M_{ash} is the mass of the sample after combustion process (g), and M_{bc} is the mass oven dry biochar before combustion process.

In all laboratory work, the different standard solutions were prepared by diluting a stock solution of $Cu(NO_3)_2$ (1000 mg/L) using bidistillate water into desired concentrations by proper dilution for different experimental purposes. All the chemical reagents used in the experimental studies were analytical grade without further purification and purchased from local supplier Merck in Indonesia.

2.2. Optimization Approach Using Box-Behnken Design (BBD)

The experimental range of the selected carbonization variables as the independent variables, were determined from the previous study of the effect of carbonization parameters (Rusnam *et al*., 2024). Table 1 clearly presented the coded levels and the experimental range of all the independent variables with their units and nomenclatures.

Table 1. The coded levels and experimental range of independent variables.

Variables	Unit	Nomenclature	Range and Levels Coded		
			-1	0	+1
Temperature	ºC	X_1	450	500	550
Time	H	X_2	1	1.5	2
Gradient	ºC/min	X_3	15	20	25

The defined coded levels of the independent variables therefore were processed in Design-Expert version 13 software (Design Expert for Windows, Stat Soft, Inc, USA) to determine the matrix of BBD. A Box-Behnken design (BBD) requires fewer experiments (Box & Wilson, 1951). In this study, a total of 17 runs was accomplished in the BBD matrix model showed in Table 2, that involved three factors and three levels to develop the design of experiment (DoE). Four additional experiments were conducted to determine the repeatability of the experiments using the variable input of any one of the DoE. Table 2 indicated the experiment number and the input variables (temperature, time and gradient) combination values and the Fe ion biosorption output results that were determined experimentally, namely removal efficiency (*RE*) in %, and biosorption capacity (*qt*) in mg/g. Different biochars were obtained for each dependent variable biosorption study. Each of running was performed triplicate and the mean was analyzed.

Table 2. Coded and actual values aligned with the actual and predicted results of BBD experiments

Run	Coded values			Actual Values			Actual Results		Predicted Results	
	X_1	X_2	X_3	X_1	X_2	X_3	RE (%)	q_t (mg/g)	RE (%)	q_t (mg/g)
1	0	0	0	500	1.5	20	6.69	0.31	9.50	0.442
2	1	0	-1	550	1.5	15	28.40	1.33	28.40	1.33
3	0	-1	-1	500	1	15	11.74	0.55	11.74	0.55
4	0	0	0	500	1.5	20	9.37	0.44	9.50	0.442
5	1	1	0	550	2	20	98.9	4.61	98.9	4.61
6	-1	-1	0	450	1	20	98	4.57	98.9	4.57
7	0	1	-1	500	2	15	25.91	1.21	25.91	1.21
8	0	-1	1	500	1	25	14.18	0.66	14.18	0.66
9	1	-1	0	550	1	20	11.74	0.55	11.74	0.55
10	1	0	1	550	1.5	25	99.83	4.66	99.83	4.66
11	-1	1	0	450	2	20	97.98	4.57	97.98	4.57
12	0	0	0	500	1.5	20	9.00	0.42	9.50	0.442
13	0	0	0	500	1.5	20	8.85	0.41	9.50	0.442
14	0	0	0	500	1.5	20	13.59	0.63	9.50	0.442
15	0	1	1	500	2	25	18.07	0.84	18.07	0.84
16	-1	0	-1	450	1.5	15	40.87	1.91	40.87	1.91
17	-1	0	1	450	1.5	25	57.40	2.68	57.40	2.68

2.3. Biosorption Experiments

The combined influence of carbonization temperature (450 – 550 ºC), time (1-2 h) and temperature gradient (15 – 25 ºC/min) on iron removal by ECH-biochar were studied at constant heavy metal initial concentration of 50 ppm, room temperature, 2 h of contact time and shaking of 150 rpm. The biosorption studied were carried out in laboratory using ECH-biochar from carbonization process according to the BBD matrix. Each of the experiment established the output that was used in the selection of the efficiency of the iron removal. The filtration by 0.25 µm filters separated the biosorbent and liquid samples. The samples that were obtained were placed into glass containers and analyzed by an atomic adsorption spectrophotometer (AAS) (AA 7000, Shimadzu, Japan). The removal efficiency (*RE*) and biosorption capacity (*qt*) (mg/g) were determined by Equation (3) and (4) as follow:

$$RE\ (\%) = \frac{C_i - C_f}{C_i} \times 100 \quad (3)$$

$$qt\ (\text{mg/g}) = \frac{C_i - C_f}{m} \times V \quad (4)$$

where C_i and C_f are respectively the initial and final concentration (mg/L) of the Fe (II), m is mass of biochar, and V is volume of the heavy metal solution during biosorption.

To identify the optimal inputs for the Fe ion biosorption process, the sufficiency of the devised model and statistical significance of the regression coefficients were evaluated by applying the analysis of variance (ANOVA). The experimental values of the dependent variables were analyzed using Design-Expert version 13 software (Design Expert for Windows, Stat Soft, Inc, USA). Furthermore, the form statistical techniques that require the use of a regression model that consists of a low-degree polynomial function (Equation 5) is often taken by RSM. In the polynomial, Y is an experimental response or output, e is the error, X_1, X_2, X_3…, X_k are input parameters and f consists of cross products of polynomial terms.

$$Y = f(X_1, X_2, X_3, \ldots, X_k) + e \quad (5)$$

2.4. ECH Characterization

The characterization of ECH biochar samples involved a comprehensive analysis of their surface morphology and elemental composition. A Scanning Electron Microscope with energy dispersive X-Ray (SEM-EDX JEOL JSM-6510 LA) was employed for scanning, while the physical properties and atomic composition were determined through X-Ray diffraction analysis (XRD) utilizing the PANalytical X'Pert PRO series X-ray (powder) diffractometer (PANalytical, the Netherlands). Concurrently, the elucidation of functional groups present on the surface was conducted using an IRTracer-100 Fourier Transform Infrared Spectrophotometer (FT-IR) (Shimadzu, Japan).

3. RESULTS AND DISCUSSION

3.1. Yield and Ash Content

The yield and ash content of the produced biochar(s) at considering carbonization parameters were varied as presented in Table 3. The results implied that Exhausted Coffee Husk (ECH) reacted and degraded to the desired conditions differently. Overall biochar yields at the considering conditions were found to range from 27.12% to 32.66 %. Examples from the literature of biochar using different type of biomass showed that yield being dependent to time (Üner & Bayrak, 2018), temperature (Ahmad *et al*., 2012; Sun *et al*., 2014), and temperature gradient (Mohanty *et al*., 2013). Meanwhile, the ash content fell within the range of 9.17 – 18.48 %. It was noticed that the lowest ash content was from the ECH-BC at temperature of 500 °C, while the highest ash content from the experimental results was obtained from the highest temperature applied of 550 °C.

Table 3. Percentage of yield and ash content of the various ECH biochar underwent different parameters during carbonization.

Run	Coded values			Actual Values			Yield (%)	Ash (%)
	X_1	X_2	X_3	X_1	X_2	X_3		
1	0	0	0	500	1.5	20	29.89	11.14
2	1	0	-1	550	1.5	15	29.50	13.47
3	0	-1	-1	500	1	15	28.81	9.17
4	0	0	0	500	1.5	20	29.89	11.14
5	1	1	0	550	2	20	27.12	18.48
6	-1	-1	0	450	1	20	28.96	10.00
7	0	1	-1	500	2	15	27.29	10.31
8	0	-1	1	500	1	25	28.30	11.78
9	1	-1	0	550	1	20	28.96	17.03
10	1	0	1	550	1.5	25	27.06	14.96
11	-1	1	0	450	2	20	30.10	10.11
12	0	0	0	500	1.5	20	29.89	11.14
13	0	0	0	500	1.5	20	29.89	11.14
14	0	0	0	500	1.5	20	29.89	11.14
15	0	1	1	500	2	25	26.55	10.35
16	-1	0	-1	450	1.5	15	32.66	9.18
17	-1	0	1	450	1.5	25	31.52	9.23

The data from the experiments, which focused on yield and ash content, indicated that increasing the temperature and duration of carbonization resulted in a reduced production of biochar. Therefore, a lack of optimal conditions was observed. Optimizing the parameters of carbonization is essential not only to determine an efficient carbonization process but also to enhance the removal of Fe ions effectively.

3.2. Batch Biosorption Studies

The ECH underwent the carbonization process considering the actual values of carbonization parameters applied in 17 runs prior to conducting the biosorption studies. The RE and qt of ECH biochar(s) obtained from the 17 carbonization runs on Fe ion were given in Table 2. In addition to actual values from experimental studies, the predicted values were also shown in the Table 2. The combined influence of the interaction of two parameters were given the below section.

- Combined Consequences of Temperature × Time

The combined effect of temperature (450 – 550 ºC) and time (1 – 2 h) of ECH carbonization on Fe removal by using biochar was studied at constant initial concentration of the heavy metal, initial pH of the solution of heavy metal, and biosorption time and rpm. While the two parameters were varied, the gradient applied was constant during carbonization before the biochar was used in the biosorption experiments. The RSM diagram on *RE* and *qt* were presented in Figure 1*a* and 1*b*, respectively. In the present study, the maximum removal percentage and biosorption capacity were found to be 98.9 at temperature of 550 ºC and time of 2 h. At the higher temperature of biomass carbonization, the formed biochar mostly provided better (Huang *et al*., 2021; Üner & Bayrak, 2018).

It was clearly seen in Table 2, the increasing temperature of 450 ºC - 550 ºC resulted in the increasing RE and qt, from 97.98 to 98.9 and 4.57 to 4.61 mg/g, respectively. The RE and qt went down when the temperature increased from 450 ºC to 500 ºC before risen up when the temperature increased from 500 ºC to 550 ºC. The interesting finding was related to the pores formation as discussed in the previous study by Üner & Bayrak (2018). Theoretically, more pores would be formed when temperature increase, however in this study, the temperature increased to 500 ºC could be resulted in bigger pores but with lower surface area which resulted in lower RE as stated in the previous study of Nilavazhagi & Felixkala (2021). However, when the temperature increased from 500 ºC to 550 ºC, the pores restructuring could be happening, which could result in biochar with higher surface area porous and gave a higher RE and qt on Fe ion removal.

- Combined Consequences of Temperature × Gradient

The temperature has been reported frequently as the most important effect on biomass carbonization as biosorbent for heavy metal ion removal. However, not many study has reported the effect of gradient during carbonization of biomass. The combined effect of temperature (450 – 550 ºC) and gradient (15 – 25 ºC/min) on Fe ion removal was deliberated at a constant initial concentration, initial pH of the solution, and biosorption time and rpm. When the combined effect of temperature and gradient was studied, the time was kept constant of 2h and the RSM diagram was presented in the Figures 1*c* and 1*d*. In the present investigation, the maximum *RE* and *qt* obtained were 99.83% and 4.66 mg/g, respectively. The maximum removal was exhibited when the temperature was 550 ºC and the gradient was 25 ºC/min. It was clearly seen from the table 2, at the maximum temperature of 550 ºC, the *RE* rose from 28.4% to 99.83% when the gradient increased from 15 ºC/min to 25 ºC/min. Compared to the combination effect of temperature and time, the combination of temperature and gradient resulted in slightly higher maximum *RE* and *qt*.

- Combined Consequences of Time × Gradient

The interplay between carbonization time and gradient is one of the key variables on the carbonization process of ECH biochar. The combined outcome of the two parameters on Fe ion removal by ECH-biochar was investigated at constant initial concentration, initial pH of the solution, and biosorption time and rpm. The temperature applied was constant at the varied time (1-2 h) and gradient (15 -25 ºC/min) during carbonization, before the biochar was used in the biosorption experiments. It was revealed in the current study that the maximum *RE* (Figure 1*e*) and *qt* (Figure 1*f*) of the combination parameters was 18.07% and 0.84 mg/g, respectively. The combination effect of the two parameters were resulted in significantly lower *RE* and *qt* compared to the other two combination effects.

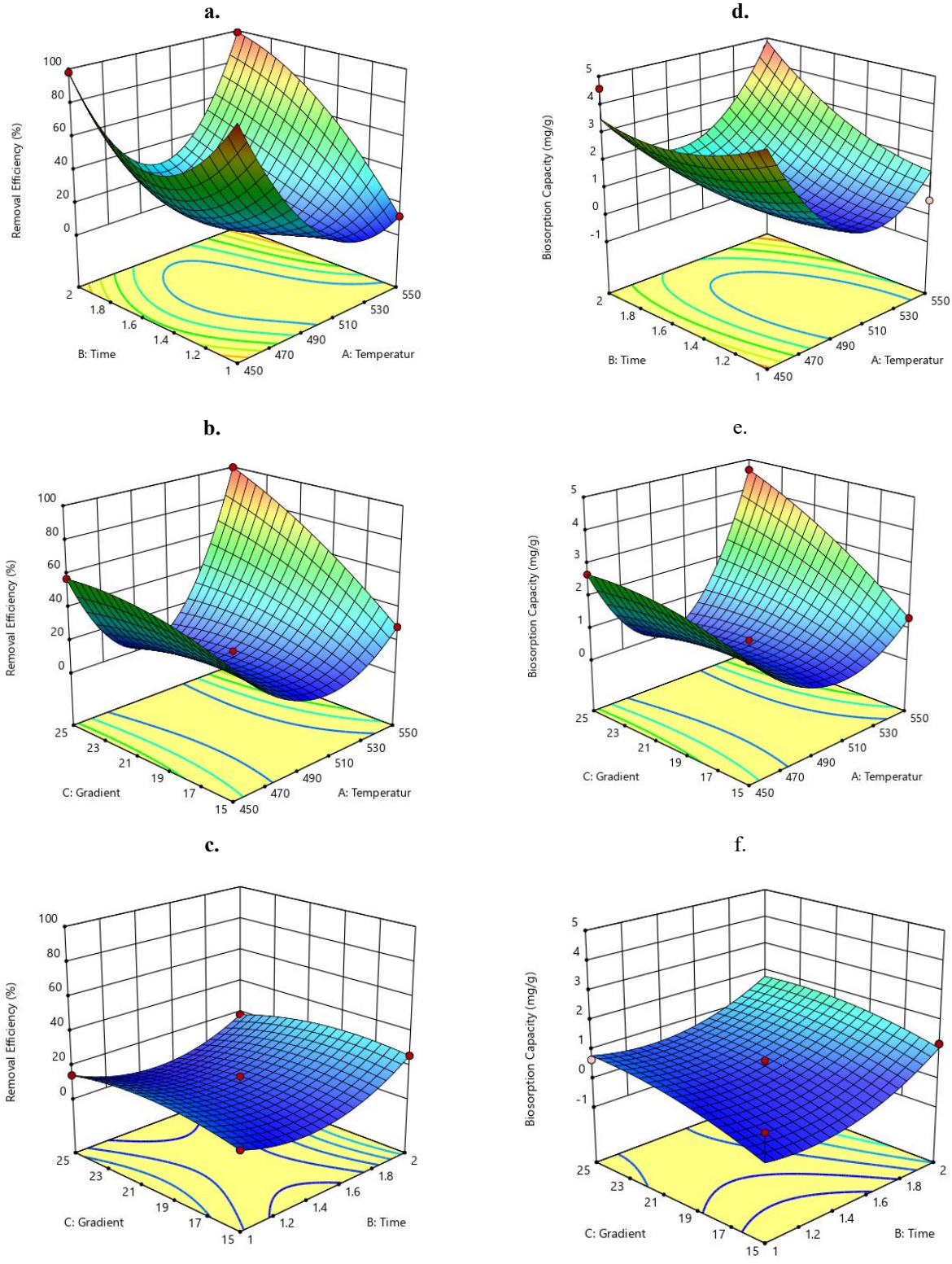

Figure 1. Three-dimensional (3D) response surface plots of the interaction of a) temperature (X1) and time (X2), b) temperature (X1) and gradient (X3) c) time (X2) and gradient (X3) for removal effiency; d) temperature (X1) and time (X2), e) temperature (X1) and gradient (X3) f) time (X2) and gradient (X3) for biosorption capacity.

3.3. Box-Bhenken Design (BBD) and Analysis

• Analysis of Variance (ANOVA)

The analysis of Variance (ANOVA) was conducted to evaluate the statistical importance of the surface response quadratic model. The quadratic regression model for RE and qt were written in Equation (6) and (7), respectively. The model showed *p*-value <0.05, while the correlation coefficient of R^2 and the R^2_{adj} of the models were 0.9393 and 0.8614, respectively. Referring to Zhou *et al*. (2019), the R^2 and the R^2_{adj} from this study indicated that the regression model could fit the experimental data. Table 4 displayed the ANOVA results of the obtained quadratic models. Apparently in the Table, the p-value of most input parameters and their combinations were more than 0.05. Furthermore, lack of fit showed a significant result of p-value which indicated that the second order model was not fitted all the experimental data.

Table 4. The quadratic regression model of ANOVA for removal efficiency and biosorption capacity of Fe^{2+} by ECH-BC.

Source	Sum of Squares	Df	Mean Square	F-value	p-value Prob > F
Removal Efficiency (%)					
Model	21814.29	9	2423.81	12.05	0.0017
X_1- Temperature	74.42	1	72.42	0.3599	0.5675
X_2 - Time	92.75	1	92.75	0.4609	0.5190
X_3 - Gradient	937.23	1	937.23	4.66	0.0678
X_1X_2	20.75	1	20.75	0.1031	0.7575
X_1X_3	825.41	1	825.41	4.10	0.0825
X_2X_3	26.68	1	26.68	0.1326	0.7265
X_1^2	16005.64	1	16005.64	79.54	<0.0001
X_2^2	2434.87	1	2434.87	12.10	0.1013
X_3^2	1290.95	1	1290.95	6.42	0.0391
Residual	1408.57	7	201.22		
Lack of Fit	1383.76	3	461.25	74.36	0.0006
Pure Error	24.81	4	6.20		
Cor Total	23222.86	16			
Biosorption Capacity (q_t)					
Model	50.57	9	5.62	14.04	0.0011
X_1- Temperature	0.2048	1	0.1352	0.3377	0.5794
X_2 - Time	1.86	1	0.2048	0.5116	0.4976
X_3 - Gradient	0.0484	1	1.86	4.65	0.0679
X_1X_2	1.64	1	0.0484	0.1209	0.7383
X_1X_3	0.0576	1	1.64	4.09	0.0828
X_2X_3	35.79	1	0.0576	0.1439	0.7157
X_1^2	6.80	1	35.79	89.41	<0.0001
X_2^2	3.92	1	6.80	16.98	0.0045
X_3^2	2.80	1	3.92	9.78	0.0167
Residual	2.76	7	0.4003	-	-
Lack of Fit	2.64	3	0.9206	90.87	0.0004
Pure Error	0.0405	4	0.0101	-	-
Cor Total	53.37	16	-	-	-

$$Y_{RE}(\%) = 10.47 + 3.01X_1 + 3.41X_2 - 10.82X_3 + 2.28X_1X_2 + 14.37X_1X_3 - 2.58X_2X_3 + 61.66\,X_1^{\,2} + 24.05X_2^{\,2} - 17.51X_3^{\,2} \quad (6)$$

$$Y_{qt}(\text{mg/g}) = 0.484 + 0.13X_1 + 0.16X_2 - 0.4825X_3 + 0.11X_1X_2 + 0.64X_1X_3 - 0.12X_2X_3 + 2.92X_1^{\,2} + 1.27X_2^{\,2} - 0.9645X_3^{\,2} \quad (7)$$

Table 5. The cubic regression model of ANOVA for removal efficiency and biosorption capacity of Fe^{2+} by ECH-BC.

Source	Sum of Squares	Df	Mean Square	F-value	p-value Prob > F
Removal Efficiency (%)					
Model	23198.05	12	1933.17	311.67	< 0.0001
X_1- Temperature	245.55	1	245.55	39.59	0.0033
X_2 - Time	82.54	1	82.54	13.31	0.0218
X_3 - Gradient	7.37	1	7.37	1.19	0.3369
$X_1 X_2$	20.75	1	20.75	3.35	0.1414
$X_1 X_3$	825.41	1	825.41	133.08	0.0003
$X_2 X_3$	26.68	1	26.68	4.30	0.1068
X_1^2	16005.64	1	16005.64	2580.47	< 0.0001
X_2^2	2434.87	1	2434.87	392.56	< 0.0001
X_3^2	1290.95	1	1290.95	208.13	0.0001
$X_1 X_2 X_3$	0.0000	0			
$X_1^2 X_2$	10.35	1	10.35	1.67	0.2660
$X_1^2 X_3$	1187.06	1	1187.06	191.38	0.0002
$X_1 X_2^2$	186.34	1	186.34	30.04	0.0054
$X_1 X_3^2$	0.0000	0			
$X_2^2 X_3$	0.0000	0			
$X_2 X_3^2$	0.0000	0			
X_1^3	0.0000	0			
X_2^3	0.0000	0			
X_3^3	0.0000	0			
Pure Error	24.81	4	6.20		
Cor Total	23222.86	16			
Biosorption Capacity (q_t)					
Model	53.33	12	4.44	438.70	< 0.0001
X_1- Temperature	0.4900	1	0.4900	48.37	0.0022
X_2 - Time	0.1764	1	0.1764	17.41	0.0140
X_3 - Gradient	0.0144	1	0.0144	1.42	0.2990
$X_1 X_2$	0.0484	1	0.0484	4.78	0.0941
$X_1 X_3$	1.64	1	1.64	161.74	0.0002
$X_2 X_3$	0.0576	1	0.0576	5.69	0.0756
X_1^2	35.79	1	35.79	3533.08	< 0.0001
X_2^2	6.80	1	6.80	670.93	< 0.0001
X_3^2	3.92	1	3.92	386.66	< 0.0001
$X_1 X_2 X_3$	0.0000	0			
$X_1^2 X_2$	0.0200	1	0.0200	1.97	0.2327
$X_1^2 X_3$	2.35	1	2.35	232.42	0.0001
$X_1 X_2^2$	0.3872	1	0.3872	38.22	0.0035
$X_1 X_3^2$	0.0000	0			
$X_2^2 X_3$	0.0000	0			
$X_2 X_3^2$	0.0000	0			
X_1^3	0.0000	0			
X_2^3	0.0000	0			
X_3^3	0.0000	0			
Pure Error	0.0405	4	0.0101		
Cor Total	53.37	16			

As the quadratic model was not fitted, therefore the cubic regression model was used. The cubic regression equation was shown in Equation (8) and (9), and the ANOVA for removal efficiency (*RE*) and biosorption capacity (*qt*) were listed in Table 5. The *F*-value of the model for *RE* and qt were 311.67 and 438.70, respectively. The values were higher than the ones from quadratic regression (Table 4), which means that the cubic regression model was more fitted than the quadratic one. Meanwhile, the correlation coefficient of R^2 and the R^2_{adj} from the cubic regression model

were 0.9989 and 0.9957. As presented in Table 6, these numbers were also notably higher than the numbers obtained from the quadratic regression model. Hence, comparing the ANOVA analysis of the two models, we could confirm that cubic regression model is more well-fitted for the ECH-biochar on Fe ion removal.

Table 6. The values of quadratic and cubic regression models

Regression Model	R^2	Adjusted R^2	SNR
Quadratic	0.9393	0.8614	9.6205
Cubic	0.9989	0.9957	41.0261

$$Y_{RE}(\%) = 10{,}47 + 7{,}84X_1 + 4{,}54X_2 - 1{,}36X_3 + 2{,}28X_1X_2 + 14{,}37X_1X_3 - 2{,}58X_2X_3 + 61{,}66\,X_1^2 + 24{,}05X_2^2 - 17{,}51X_3^2 - 2{,}27X_1^2X_2 + 24{,}36X_1^2X_3 - 9{,}65X_1X_2^2 \quad (8)$$

$$Y_{qt}(\mathrm{mg/g}) = 0{,}484 + 0{,}35X_1 + 0{,}21X_2 - 0{,}06X_3 + 0{,}11X_1X_2 + 0{,}64X_1X_3 - 0{,}12X_2X_3 + 2{,}92\,X_1^2 + 1{,}27X_2^2 - 0{,}9645X_3^2 - 0{,}1X_1^2X_2 + 0{,}1{,}09X_1^2X_3 - 0{,}44X_1X_3^2 \quad (9)$$

- Multi-Response Optimization

From the cubic multiple regression models, the response surface three-dimensional diagram of the interaction of carbonization temperature (X_1), carbonization time (X_2) and carbonization gradient (X_3) on the removal efficiency and biosorption capacity of Fe (II) adsorbed by ECH-BC can be obtained. The Figure 1 (*a-f*) showed the response surface three-dimensional diagram of the results.

It can be seen from Figure 1*a* and 1*d* that the response surface of carbonization temperature (X_1) and carbonization time (X_2) for removal efficiency (*RE*) and biosorption capacity (*qt*), respectively, had a steep slope, indicating significant interaction between the two parameters (Zhou *et al*., 2019). Therefore, temperature and time play a crucial role in utilizing biochar from ECH for adsorbing Fe^{2+}. It was clearly seen that their changes resulted in a common effect on Fe^{2+} biosorption by ECH-BC. As discussed in biosorption section, and looking in overall perspective in Figure 1*a* and 1*d*, when X_2 is fixed, the *RE* and *qt* changed with an increase of X_1. Meanwhile, in Figure 1*b* and 1*e*, the response surface of carbonization temperature (X_1) and carbonization gradient (X_3) for *RE* and *qt* showed a steeper slope compared to the interaction of X_1 and X_2 (Figure 1*a* and 1*d*). The comparison implied that the interaction of X_1 and X_3 had a more significant effect than X_1 and X_2, related to the biosorption performance of ECH-biochar that underwent carbonization under the interaction of the parameters.

Interestingly, in the interaction of X_1 and X_3, when the X_3 was constant at the minimum level, the *RE* and *qt* showed a considerable declined before increased back. However, the increasing was not as high as the initial one. In the meantime, when the X_3 was constant at the maximum level, the *RE* and *qt* were also showed a considerable declined and significantly increased back to the higher value than the initial one. The last interaction was in between the carbonization time (X_2) and carbonization gradient (X_3), which were shown in Figure 1*c* and 1*f*. In the figures, the response surface of the interaction did not show a slope as steep as the interaction of X_1 and X_3. This means the interaction between of gradient (X_3) with the applied temperature (X_1) has more important role that the interaction between the gradient (X_3) and the applied time (X_2). From *F*-value and *p*-value presented in the Tables 4 and 5, it can be concluded that the order of influence of interaction term on the biosorption performance of ECH-BC on Fe^{2+} is: X_1 and $X_3 > X_2$ and $X_3 > X_1$ and X_2.

Through Design-expert 13.0 software, three carbonization factors affecting the adsorption performance ECH biochar adsorbed Fe^{2+} were obtained: The optimal combination of carbonization temperature, carbonization time and carbonization gradient was 549.37 °C, 1.98 h and 21.98 °C/min, respectively. The relationship between the predicated removal efficiency (*RE*) and biosorption capacity (*qt*) and the actual ones were displayed in Figure 2 (*a*, *b*). According to analysis of RSM fitting model, the predicated *RE* and biosorption capacity *qt* were 107.01% and 5.11 mg/g, respectively.

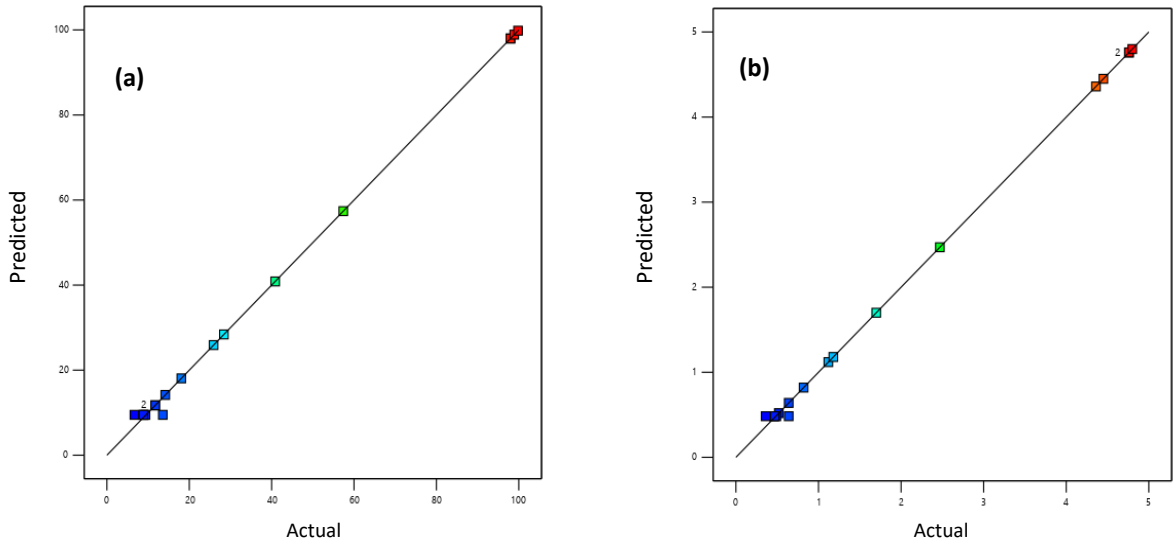

Figure 2. The relationship between predicted and actual values: (*a*) removal efficiency (*RE*), and (b) biosorption capacity (*qt*)

3.4. Characterization

• SEM-EDX

The scanning electron microscope (SEM) were obtained at 200 K x magnification embedded with energy dispersive spectrum (EDX) of the optimum ECH biochar, before and after biosorption of Fe ion were shown in Figure 3. The SEM image of the ECH-BC at optimum carbonization parameters had a smoother surface (Figure 3*b*). Previous study of Zeng *et al*. (2013) with the similar observation, mentioned the indication of micropores domination in the surface area of the material, which could be caused by the carbonization process. From Figure 3, no significant differences were found on morphological surfaces between before and after biosorption of Fe ion. However, referring to the element content of the materials of two conditions in Table 7, it was noteworthy to state that ion exchange was one of the mechanisms of Fe ion reduction by ECH biochar. In the Table 7, K and Ca were dominant elements in the ECH biochar before biosorption, followed by Zn, Cu and Mg. However, after the biosorption, the percentages of the elements were changed, where the K and Ca reduced from 3.29 to 0.3 and 1.34 to 1.01, respectively. Meanwhile, the elemental composition of Fe slightly increased after the biosorption, from 0.07 to 0.08. Aligning the EDX results with the previous study of Zhou *et al*. (2019), the results interpretation led to ion exchange phenomena as one of the mechanism of Fe removal by the ECH-BC.

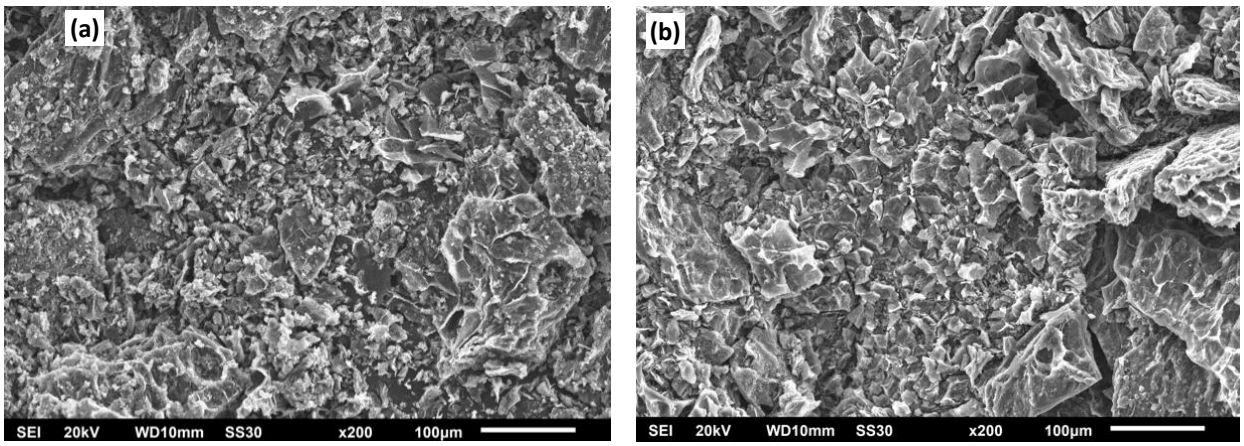

Figure 3. Scanning of surface morphology of ECH-BC: (a) before biosorption, and (b) after biosorption of Fe^{2+}.

Table 7. Elemental composition (% w/w) of ECH-BC before and after biosorption of Fe^{2+}.

Element	C	O	Mg	Si	K	Ca	Fe	Cu	Zn	Total
Before	91.31	2.06	0.37	0.13	3.29	1.34	0.07	0.61	0.83	100
After	96.05	1.06	0.50	-	0.30	1.01	0.08	0.64	0.36	100

• XRD

XRD patterns of ECH-biochar before and after underwent biosorption process on Fe^{2+} were shown in Figure 4a. It can be seen in the Figure that the ECH-BC showed a broad peak in a range of 20-30 ° and two sharp peaks in a range of 30-35 °. The broad peak was a typical of XRD pattern of biochar as also presented in the previous studies of Prasannamedha *et al*. (2021) and Nilavazhagi & Felixkala (2021). Furthermore, Muniandy *et al*. (2014) claimed the presence of peak confirms the development of microcrystalline amorphous carbon in graphitized structure. The two sharp peaks in a range of 30-35 ° was notably disappeared after the biosorption of Fe^{2+}, and new two sharp peaks were observed in a range of 20-25 °. The patterns confirmed the ion exchange phenomena as one of the mechanisms of ECH-BC biosorption on Fe^{2+}.

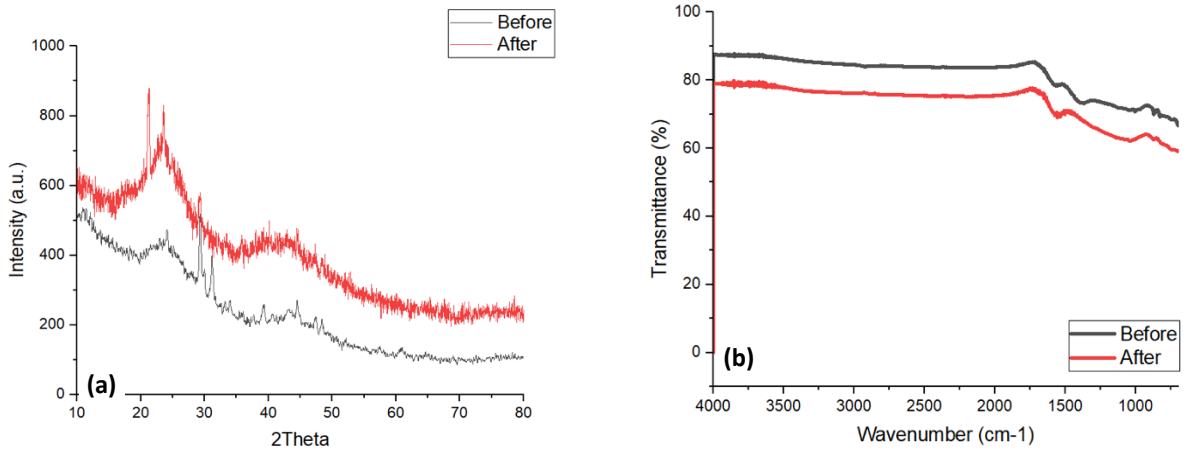

Figure 4. (a) XRD showing nature of ECH-BC before and after biosorption with Fe^{2+}, (b) FT-IR spectrum showing modified chemical structures of ECH-BC before and after biosorption with Fe^{2+}.

• FT-IR

The FTIR spectra of ECH-BC before and after biosorption were depicted in Fig. 4b. The spectra did not show significant difference of the peak in ECH-BC that underwent biosorption of Fe^{2+}. The spectrum of ECH-BC before biosorption showed a sharp and intense peak at the range of 1500 -1600 cm-1 and 1000 – 1200 cm-1 which belonged to the stretching vibrations of the –COO- and -OH. The peak was still seen after the biosorption yet with the lower intensity. According to the analysis, the adsorption of Fe^{2+} by ECH-BC is related to the –COO- and –OH functional groups which showed consistency with the study of Khosravihaftkhany *et al*. (2013).

4. CONCLUSIONS

In this study the optimization of biosorption performance of biochar derived from exhausted coffee husk (ECH), which is an agricultural waste product, with the combination of optimal carbonization parameters was investigated. The response surface methodology to predict the optimum conditions through Box-Bhenken Design experiment. The results concluded that the interaction of carbonization temperature and time has a significant role compared to the other two interactions between temperature and gradient and time and gradient. Furthermore, the cubic regression was more fit to the model compared to the quadratic regression. The regression model was used to predict the optimal values of the carbonization parameters, which the outcomes for temperature (549.37 °C), time (1.98 h), and, temperature gradient (21.98 °C/min). The predicted optimum removal efficiency (RE) and biosorption capacity (qt) of

ECH biochar on Fe2+ under the optimal carbonization were 107.01% and 5.11 mg/g, respectively. The RSM was successfully applied for the mathematical modelling of biosorption process and the predictability of the biosorption results. Additionally, SEM-EDX, XRD and FT-IR analysis were included to the characterisation of ECH-biochar to predict the mechanism of the ECH-biochar biosorption onto Fe^{2+}. Ion exchange and surface functional groups were responsible for the removal of Fe^{2+} from aqueous solution. From the results, it can be said that ECH-biochar has the potential to be used as an alternative and low-cost biosorbent to for Fe^{2+} removal in environmental remediation applications.

ACKNOWLEDGEMENT

This research was supported by the Faculty of Agricultural Technology, Andalas University, under DIPA research fund 2023. The authors would also like to thank Arti Azora and Ika for their helpful collaboration during analysis.

CONFLICT OF INTEREST

The authors declare that they have no known competing financial interests or personal relationships that could have appeared to influence the work reported in this paper.

REFERENCES

Ahmad, M., Lee, S.S., Dou, X., Mohan, D., Sung, J.K., Yang, J.E., & Ok, Y.S. (2012). Effects of pyrolysis temperature on soybean stover- and peanut shell-derived biochar properties and TCE adsorption in water. *Bioresource Technology*, ***118***, 536–544. https://doi.org/10.1016/j.biortech.2012.05.042.

Aller, D., Bakshi, S., & Laird, D.A. (2017). Modified method for proximate analysis of biochars. *Journal of Analytical and Applied Pyrolysis*, ***124***, 335–342. https://doi.org/10.1016/j.jaap.2017.01.012

Bezerra, M.A., Santelli, R.E., Oliveira, E.P., Villar, L.S., & Escaleira, L.A. (2008). Response surface methodology (RSM) as a tool for optimization in analytical chemistry. *Talanta*, ***76***(5), 965-977. https://doi.org/10.1016/j.talanta.2008.05.019

Box, G.E.P., & Wilson, K.B. (1951). On the Experimental Attainment of Optimum Conditions. *Journal of the Royal Statistical Society: Series B (Methodological)*, ***13***(1), 1-38. https://doi.org/10.1111/j.2517-6161.1951.tb00067.x.

Corral-Bobadilla, M., Lostado-Lorza, R., Somovilla-Gómez, F., & Escribano-García, R. (2021). Effective use of activated carbon from olive stone waste in the biosorption removal of Fe(III) ions from aqueous solutions. Journal of Cleaner Production, 294, 126332. https://doi.org/10.1016/j.jclepro.2021.126332.

Fu, F., & Wang, Q. (2011). Removal of heavy metal ions from wastewaters: A review. Journal of Environmental Management, 92(3), 407–418. https://doi.org/10.1016/j.jenvman.2010.11.011.

Gadd, G.M. (2008). Biosorption: Critical review of scientific rationale, environmental importance and significance for pollution treatment. *Journal of Chemical Technology and Biotechnology*, ***84***(1), 13–28. https://doi.org/10.1002/jctb.1999.

Huang, H., Reddy, N.G., Huang, X., Chen, P., Wang, P., Zhang, Y., Huang, Y., Lin, P., & Garg, A. (2021). Effects of pyrolysis temperature, feedstock type and compaction on water retention of biochar amended soil. *Scientific Reports*, ***11***(7419). https://doi.org/10.1038/s41598-021-86701-5.

Huang, J., Kankanamge, N.R., Chow, C., Welsh, D.T., Li, T., & Teasdale, P.R. (2018). Removing ammonium from water and wastewater using cost-effective adsorbents: A review. *Journal of Environmental Sciences*, ***63***, 174–197. https://doi.org/10.1016/j.jes.2017.09.009.

Jaishankar, M., Tseten, T., Anbalagan, N., Mathew, B.B., & Beeregowda, K.N. (2014). Toxicity, mechanism and health effects of some heavy metals. *Interdisciplinary Toxicology*, ***7***(2), 60–72. https://doi.org/10.2478/intox-2014-0009.

Kaçakgil, E.C., & Çetintaş, S. (2021). Preparation and characterization of a novel functionalized agricultural waste-based adsorbent for Cu^{2+} removal: Evaluation of adsorption performance using response surface methodology. *Sustainable Chemistry and Pharmacy*, ***22***(September), 100468. https://doi.org/10.1016/j.scp.2021.100468.

Khosravihaftkhany, S., Morad, N., Teng, T.T., Abdullah, A.Z., & Norli, I. (2013). Biosorption of Pb(II) and Fe(III) from aqueous solutions using oil palm biomasses as adsorbents. *Water, Air, and Soil Pollution*, ***224***(1455). https://doi.org/10.1007/s11270-013-1455-y.

Korondi, P.Z., Marchi, M., & Poloni, C. (2021). Response surface methodology. In Optimization Under Uncertainty with Applications to Aerospace Engineering. *Springer Link*, 387-409. https://doi.org/10.1007/978-3-030-60166-9_12.

Mallesh, B. (2018). A Review of Electrocoagulation Process for Wastewater Treatment. *International Journal of ChemTech Research*, 11(03), 289-302. https://doi.org/10.20902/ijctr.2018.110333.

MarouŠek, J. (2013). Removal of hardly fermentable ballast from the maize silage to accelerate biogas production. *Industrial Crops and Products*, ***44***, 253-257. https://doi.org/10.1016/j.indcrop.2012.11.022.

Mohanty, P., Nanda, S., Pant, K.K., Naik, S., Kozinski, J.A., & Dalai, A.K. (2013). Evaluation of the physiochemical development of biochars obtained from pyrolysis of wheat straw, timothy grass and pinewood: Effects of heating rate. *Journal of Analytical and Applied Pyrolysis*, ***104***, 485–493. https://doi.org/10.1016/j.jaap.2013.05.022.

Muniandy, L., Adam, F., Mohamed, A.R., & Ng, E.P. (2014). The synthesis and characterization of high purity mixed microporous/mesoporous activated carbon from rice husk using chemical activation with NaOH and KOH. *Microporous and Mesoporous Materials*, ***197***,316-323. https://doi.org/10.1016/j.micromeso.2014.06.020.

Ngah, W.S.W., Ab Ghani, S., & Kamari, A. (2005). Adsorption behaviour of Fe(II) and Fe(III) ions in aqueous solution on chitosan and cross-linked chitosan beads. *Bioresource Technology*, ***96***(04), 443-450. https://doi.org/10.1016/j.biortech.2004.05.022.

Nilavazhagi, A., & Felixkala, T. (2021). Adsorptive removal of Fe(II) ions from water using carbon derived from thermal/chemical treatment of agricultural waste biomass: Application in groundwater contamination. *Chemosphere*, ***282***(June), 131060. https://doi.org/10.1016/j.chemosphere.2021.131060.

Prasannamedha, G., Kumar, P.S., Mehala, R., Sharumitha, T.J., & Surendhar, D. (2021). Enhanced adsorptive removal of sulfamethoxazole from water using biochar derived from hydrothermal carbonization of sugarcane bagasse. *Journal of Hazardous Materials*, ***407***(November 2020), 124825. https://doi.org/10.1016/j.jhazmat.2020.124825.

Puari, A.T., Rusnam, R., & Yanti, N.R. (2022). Optimization of the carbonization parameter of exhausted coffee husk (ECH) as biochar for Pb and Cu removal based on energy consumption. *Jurnal Teknik Pertanian Lampung*, ***11***(2), 242-252. https://doi.org/10.23960/jtep-l.v11.i2.242-252.

Qasem, N.A.A., Mohammed, R.H., & Lawal, D.U. (2021). Removal of heavy metal ions from wastewater: a comprehensive and critical review. *Npj Clean Water*, ***4***(1). https://doi.org/10.1038/s41545-021-00127-0.

Rusnam, R., Puari, A.T., Yanti, N.R., & Efrizal, E. (2022). Utilisation of exhausted coffee husk as low-cost bio-sorbent for adsorption of Pb^{2+}. *Tropical Life Science Research*, ***33***(3), 229–252. https://doi.org/https://doi.org/10.21315/tlsR2022.33.3.12

Rusnam, R., Yanti, N.R., Puari, A.T., & Sari, N. (2024). Application of Agro-industrial Solid Waste as Biochar for Iron (II) Removal from Aqueous Solution., *Jurnal Teknik Pertanian Lampung*, ***13***(1), 155–164. http://dx.doi.org/10.23960/jtep-l.v13i1.155-164

Sun, Y., Gao, B., Yao, Y., Fang, J., Zhang, M., Zhou, Y., Chen, H., & Yang, L. (2014). Effects of feedstock type, production method, and pyrolysis temperature on biochar and hydrochar properties. *Chemical Engineering Journal*, ***240***, 574–578. https://doi.org/10.1016/j.cej.2013.10.081.

Üner, O., & Bayrak, Y. (2018). The effect of carbonization temperature, carbonization time and impregnation ratio on the properties of activated carbon produced from *Arundo donax*. *Microporous and Mesoporous Materials*, ***268***(March), 225–234. https://doi.org/10.1016/j.micromeso.2018.04.037.

Zeng, Z., Zhang, S. Da, Li, T. Q., Zhao, F.L., He, Z.L., Zhao, H.P., Yang, X.E., Wang, H.L., Zhao, J., & Rafiq, M.T. (2013). Sorption of ammonium and phosphate from aqueous solution by biochar derived from phytoremediation plants. *Journal of Zhejiang University: Science B*, ***14***(12), 1152–1161. https://doi.org/10.1631/jzus.B1300102.

Zhou, R., Zhang, M., Zhou, J., & Wang, J. (2019). Optimization of biochar preparation from the stem of *Eichhornia crassipes* using response surface methodology on adsorption of Cd^{2+}. *Scientific Reports*, ***9***(1), 1–17. https://doi.org/10.1038/s41598-019-54105-1.